



Temperature persistent bistability and threshold switching in a single barrier heterostructure hot-electron diode

Stasch, R.; Hey, R.; Asche, M.; Wacker, Andreas; Schöll, E.

Published in:
Journal of Applied Physics

Link to article, DOI:
[10.1063/1.363251](https://doi.org/10.1063/1.363251)

Publication date:
1996

Document Version
Publisher's PDF, also known as Version of record

[Link back to DTU Orbit](#)

Citation (APA):
Stasch, R., Hey, R., Asche, M., Wacker, A., & Schöll, E. (1996). Temperature persistent bistability and threshold switching in a single barrier heterostructure hot-electron diode. *Journal of Applied Physics*, 80(6), 3376-3380. <https://doi.org/10.1063/1.363251>

General rights

Copyright and moral rights for the publications made accessible in the public portal are retained by the authors and/or other copyright owners and it is a condition of accessing publications that users recognise and abide by the legal requirements associated with these rights.

- Users may download and print one copy of any publication from the public portal for the purpose of private study or research.
- You may not further distribute the material or use it for any profit-making activity or commercial gain
- You may freely distribute the URL identifying the publication in the public portal

If you believe that this document breaches copyright please contact us providing details, and we will remove access to the work immediately and investigate your claim.

Temperature persistent bistability and threshold switching in a single barrier heterostructure hot-electron diode

R. Stasch, R. Hey, and M. Asche^{a)}
Paul-Drude-Institut, Hausvogteiplatz 5-7, D-10117 Berlin, Germany

A. Wacker
Mikroelektronik Centret, Technical University of Denmark, DK-2800 Lyngby, Denmark

E. Schöll
Institut für Theoretische Physik, Technische Universität Berlin, Hardenbergstrasse 36, D-10623 Berlin, Germany

(Received 27 February 1996; accepted for publication 11 June 1996)

Bistable current–voltage characteristics caused by competition of tunneling through and field-enhanced thermionic emission across a single barrier are investigated in an n^- -GaAs/Al_{0.34}Ga_{0.66}As/ n^+ -GaAs structure. The S-shaped part of the characteristic persists in the whole temperature regime between 4.2 and 300 K in accordance with theoretical predictions. The delay and switching times of the transition from the low- to the high-conducting state are investigated as a function of the applied voltage and compared with simulations. The observed timescales are much longer than expected from theory, which indicates the presence of additional deep centers or interface states. © 1996 American Institute of Physics. [S0021-8979(96)04418-0]

I. INTRODUCTION

Semiconductor heterostructures are well known to exhibit various types of electric instabilities if a sufficiently high bias is applied.¹ A simple structure, which exhibits an S-shaped current–voltage characteristic under certain conditions, is the heterostructure hot-electron diode (HHED), which consists of a single barrier clad between lightly and heavily doped smaller gap semiconductor layers.² At a given voltage applied perpendicular to the heterolayers, bistability is possible if the current is carried predominantly either by tunneling through the barrier (low-conductivity state) or by field-enhanced thermionic emission over the barrier (high-conductivity state). Switching between these two steady states is associated with a concomitant rearrangement of the potential and charge distributions perpendicular to the junction. Regardless of the large power dissipation of the HHED, it serves as a prototype of a bistable device, which allows a convenient study of the fundamental nonlinear transport properties due its simplicity.

To the best of our knowledge there is only one experimental observation of an S-shaped characteristic of an HHED fabricated from a GaAs/Al_{0.45}Ga_{0.55}As structure² besides one from GaAs/AlAs,³ i.e., both differed in the offsets of the lowest conduction band in the barrier. It should be noted that the structure with a single barrier must be contrasted to quantum wells formed by a narrow gap semiconductor clad between layers of a wide gap semiconductor or multiple quantum wells.^{4–6} In these structures the S-shaped characteristics are due to the additional effect of energy transfer between the carriers entering the well across the barrier and those localized in the well.⁷

Theoretically the HHED has been investigated by different approaches for various choices of relevant sample parameters. In Refs. 8 and 9 Monte Carlo (MC) simulations exhib-

ited a steep increase of the current due to the onset of thermionic emission as a response to an ideal voltage source. The occurrence of an S-shaped current–voltage characteristic and consequent instabilities leading to self-sustained current oscillations were theoretically first described by a simple drift model.¹⁰ Later MC simulations also exhibited clearly pronounced hysteresis and accompanying oscillatory behavior.^{11,12}

The negative differential conductivity regime of the current–voltage characteristic was reported to vanish at temperatures above 77 K for the MOCVD-grown sample considered in Ref. 2. In contrast to this result, calculations based on an improved drift model using quasiballistic transport¹³ indicated only a moderate reduction of the bistability regime of the characteristic with increasing temperature.¹⁴ The purpose of this paper is to present experimental evidence that an S-shaped current–voltage characteristic associated with the fundamental mechanisms of tunneling and field-enhanced thermionic emission can indeed be observed in a carefully designed GaAs/Al_{0.34}Ga_{0.66}As/GaAs structure (as described below) in a wide temperature regime ranging from liquid He to room temperature. Further emphasis is placed on the dynamics of threshold switching to the high conductivity branch, since the dynamical behavior is important for applications as well as for information concerning the structural perfection of the sample.

The paper is organized as follows. In Sec. II the HHED structure and the sample preparation are described. The experimental setup and the obtained results are presented in Sec. III. In Sec. IV we discuss the temperature dependence and the dynamic behavior and draw a comparison with further numerical simulations on the basis of the model of Refs. 13 and 14.

II. STRUCTURE AND SAMPLE PREPARATION

The structure was grown by molecular beam epitaxy as indicated in Fig. 1. On an untilted n^+ GaAs (001) substrate a

^{a)}Electronic mail: asche@pdi.wias-berlin.de

GaAs:Si	$1 \times 10^{18} \text{ cm}^{-3}$	300 nm
GaAs		3 nm
$\text{Al}_{0.34}\text{Ga}_{0.66}\text{As}$		200 nm
GaAs		3 nm
GaAs:Si	$5 \times 10^{15} \text{ cm}^{-3}$	500 nm
GaAs:Si	$1 \times 10^{18} \text{ cm}^{-3}$	500 nm
GaAs:Si	$1 \times 10^{18} \text{ cm}^{-3}$	5 nm
AlAs:Si	$1 \times 10^{18} \text{ cm}^{-3}$	5 nm
GaAs:Si	$1 \times 10^{18} \text{ cm}^{-3}$	100 nm
n^+ -GaAs substrate		

FIG. 1. Scheme of the n^- -GaAs/ $\text{Al}_{0.34}\text{Ga}_{0.66}\text{As}/n^+$ -GaAs heterostructure hot electron diode (HHED).

highly doped buffer layer system including a strongly doped superlattice was grown. The superlattice is used because it is effective for smoothing of the growth front as well as for trapping of impurities from the substrate surface. The active layers of the HHED consist of 500 nm GaAs:Si ($5 \times 10^{15} \text{ cm}^{-3}$), 200 nm $\text{Al}_{0.34}\text{Ga}_{0.66}\text{As}$ and a highly doped GaAs cap layer. To avoid Si segregation into the barrier, 3 nm thick undoped GaAs layers were inserted on both sides of the barrier. The weakly doped GaAs drift region was intentionally grown in front of the barrier in order to achieve a more perfect interface for the electrons impinging on the barrier from the cathode side, than the inverse sequence would give. The substrate temperature was 600 °C, and growth was performed under arsenic stable conditions.

The lateral geometry of the samples was defined by ion implantation. At the beginning Au:Ge was evaporated, photolithographically structured, and alloyed at 470 °C. The diameters of the active regions were chosen between 30 and 6 μm for the alloyed metal contacts on the anode side. Then the contact areas were covered by deposition of a 3.5 μm thick organic sheet in order to shield the active areas against ion implantation for insulation of the surrounding. The diameter of the shielded areas were chosen 2 μm wider than the alloyed contacts. To achieve insulation of the desired parts of the cap layer the ion implantation was performed with oxygen starting with an initial energy of 220 or 180 keV and diminishing it step wise down to 25 keV. As known these upper energy limits yield a penetration of the O^+ ions of 350 and 300 nm, respectively. Note that there is no significant influence on the obtained current–voltage characteristics within this penetration range. After the implantation the protecting organic layer was removed and larger metallic areas than the defined active ones were evaporated and slightly alloyed for bonding. For this type of preparation of the anode side, the cathode was prepared on the backside of the sample. Thus the current had to pass through the whole structure.

In the experimental investigations we used smaller-diameter HHEDs in order to limit the current through the sample thus avoiding destruction of the samples at high currents.

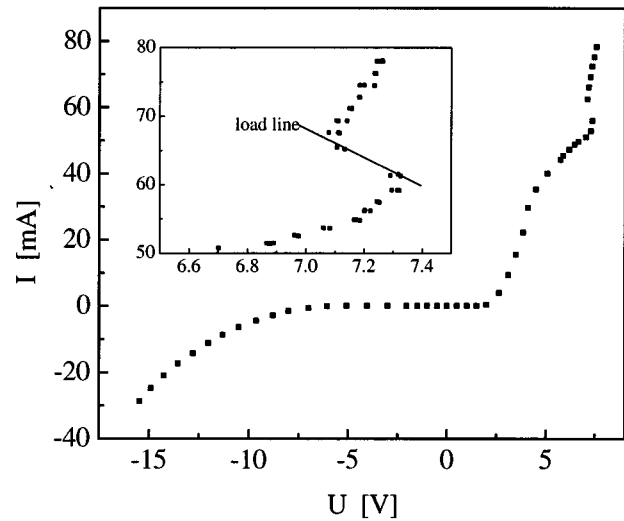


FIG. 2. Current–voltage characteristic at 4.2 K for a sample with a diameter of $d=8 \mu\text{m}$ defined by ion implantation. The widths of the drift region and the barrier are 500 and 200 nm, respectively. The inset shows the S-shaped part of the characteristic for repeated measurements.

III. EXPERIMENTAL RESULTS

The measurements were performed by rectangular voltage pulses of typically 400 ns duration and a repetition frequency of 2 Hz. A 50 Ω resistor R_1 was mounted in series with the sample to measure the current I . In order to vary the load line an additional resistor R_2 was used. For an applied voltage U_0 the voltage drop U across the sample is determined by Kirchhoff's law $U = U_0 - (R_1 + R_2)I$. The voltage drops U across the sample as well as $(R_1 + R_2)I$ were measured by a high impedance probe. The shortest pulses were about 100 ns, limited by the generator. Both the voltage and current pulses were measured at the end of the pulse, where jitter and reflections due to mismatch did not significantly influence the pulse shape. In this flat section about 150 points were measured and averaged over 20 pulses, i.e., an integration over 3000 values was performed for each value of the applied voltage. The investigations were performed either in a He gas atmosphere between 4.2 and 300 K or in liquid He, liquid nitrogen, and air, respectively.

The current–voltage characteristic for both polarities is shown in Fig. 2. In the low voltage regime it clearly demonstrates the behavior of a diode. However, at about 7 V for forward bias, i.e., for carriers drifting through the weakly doped GaAs region to the barrier a peculiarity is observed. The precise value of this critical voltage differs for samples with different diameters. It is found to shift to higher values with increasing diameter of the samples. The inset of Fig. 2 shows the S-shaped peculiarity. It can be seen that repetition of the measurement cycle has almost no influence even after long interruption intervals. It should be mentioned that the currents do not fully scale with the nominally active cross section (the current densities are reduced up to 15% with increasing cross section). This difference, however, is too small to allow for definite conclusions concerning the formation of current filaments. In fact, theoretical results suggest

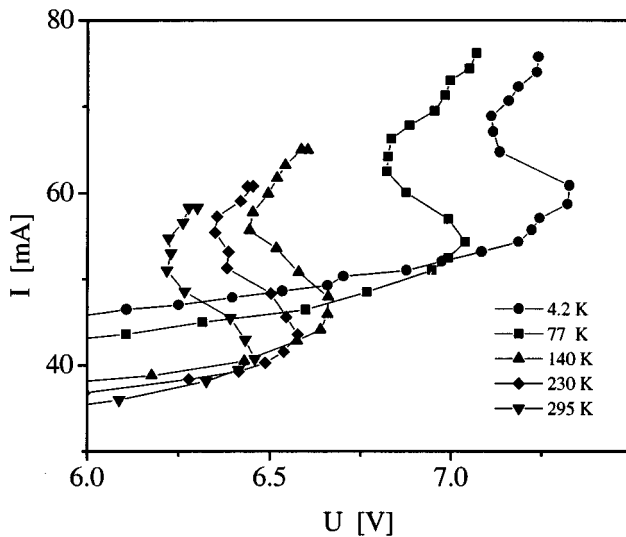


FIG. 3. S-shaped parts of the current–voltage characteristics for different lattice temperatures from 4.2 to 300 K (same sample as in Fig. 2).

that current filamentation should set in only at larger sample diameters of the order of $50 \mu\text{m}$. Note that experimentally no hysteresis is observed directly, since the measurements are performed by pulse technique.

The curves demonstrate quite clearly the occurrence of two different conducting states for a fixed sample voltage at 4.2 K. Since it is very interesting whether this behavior remains up to room temperature, we have investigated the temperature dependence in detail. As shown in Fig. 3 the threshold voltage and the current density shift to lower values with increasing lattice temperature, but the S-shaped characteristics remain up to room temperature and the bistability range is not reduced. Sweeping the temperature several times between 300 and 4.2 K yields reproducible results. The “precise” value of the critical voltage for the onset of the bistability depends on the position of the time interval chosen to determine the pulse amplitudes. This behavior is demonstrated in Fig. 4, where the temporal evolution of the current signal is shown for stepwise increased generator voltage. We stress that the generator voltage U_{gen} is different from U_0 due to electrical reflections: $U_{\text{gen}} = U_0(1 + \rho)$, where ρ denotes the reflection coefficient with $-1 \leq \rho \leq 1$. It can be seen that for earlier times of sampling a slightly higher value of applied voltage is necessary in order to attain the high-conducting state. The time traces show that the current jumps from the low-conducting to the high-conducting state (switching) occur only after some delay time, which becomes shorter when the generator voltage is slightly increased. The switching time¹⁵ can be estimated by the present setup to be about 10 ns, which is well above the experimental resolution. Note that the delay as well as the switching times slightly differ from sample to sample.

In order to study the dynamical behavior in more detail, we have plotted the delay times as a function of the generator voltage in a semilogarithmic scale in Fig. 5. The delay times decrease exponentially with increasing voltage in the regime shown. Near the turning point of the characteristic, i.e., for

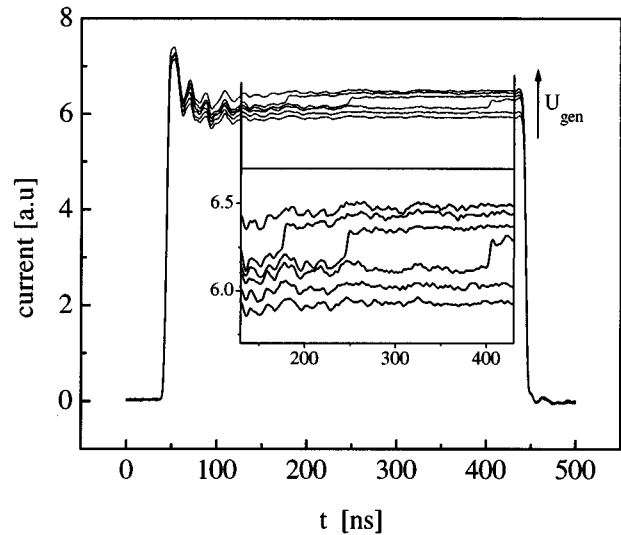


FIG. 4. Evolution of the current with time for stepwise increased generator voltage at $T=4.2 \text{ K}$ for a sample with $d=12 \mu\text{m}$ defined by ion implantation. Note that the reflection coefficient ρ was positive for these measurements.

small overvoltages, there is a stochastic regime with longer average delay times as generally expected for threshold switching.¹⁶ In this regime there are large statistical fluctuations of the delay times for a given applied voltage.

IV. DISCUSSION AND COMPARISON WITH THEORY

Our experimental investigations of the HHED clearly demonstrate the persistence of bistability between a low- and a high-conductivity branch in the whole investigated temperature regime from 4.2 up to 300 K. This agrees well with the results from the quasiballistic drift model of Refs. 13 and 14.

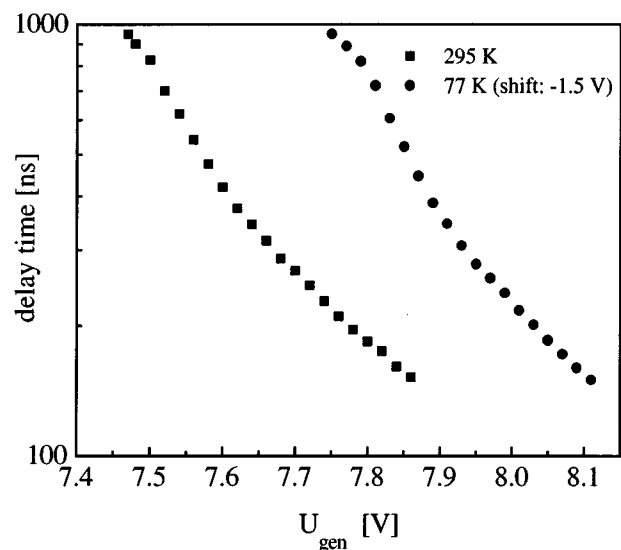


FIG. 5. Delay time of the threshold switching vs generator voltage measured for a point in the low-conducting state (Fig. 4).

The use of such a simplified transport model has the great advantage that the behavior can be easily studied in a large parameter range, for various initial conditions, and also spatiotemporal phenomena can be investigated. In contrast to this, MC simulations require a large numerical effort. Therefore, it is not surprising that a full bistability could not be resolved in Ref. 8 (which would require the use of different initial conditions) but only a switching was found. The observation of the full S-shaped curve within a MC simulation requires the use of current controlled conditions as the middle branch is unstable for voltage-controlled conditions (see, e.g., Ref. 17). Further MC simulations¹² performed for increasing as well as decreasing voltage ramps yield hysteresis and accompanying oscillations. The steepness of the transitions between the low- and the high-conducting branch is shown to depend on the Γ - L and Γ - X scattering processes. Note that for the parameters used there (short drift and barrier regions) the quasiballistic drift model does not exhibit any bistability.¹⁴

Here we will use the results of the model from Refs. 13 and 14 for a comparison with the experimental results. This model is based on quasiballistic transport in the lightly or undoped GaAs drift region. Additionally, an energy broadening of the electron distribution due to scattering with polar optical phonons and scattering into the L valley is treated as a perturbative effect. The lattice temperature mainly influences the scattering, but also the tunneling via the carrier distribution in the states bound in the triangular potential well in front of the interface. The model assumptions can only be justified for drift regions of up to roughly 200 nm, because scattering becomes much more important for longer length scales. Therefore, the model does not directly apply to our experimental situation. Nevertheless, a formal extension beyond this limit yields similar current-voltage characteristics.

The calculated current-voltage characteristics for a 200 nm GaAs drift layer are shown in Fig. 6 for 300 and 4 K. Qualitatively, they reflect the same shift with lattice temperature as experimentally observed. The range of currents and voltages at the instability are also in good qualitative agreement. The quantitative differences may be caused by the different lengths of the drift regions in theory and experiment. Furthermore, the drift region was assumed to be undoped in the simulation. Besides, the measured voltages include additional contact and substrate as well as buffer resistances and should in general be larger than the theoretical values. The strong influence of scattering events in our samples with their long drift region is clearly reflected by the sublinear current-voltage characteristic preceding the bistability regime. This may be attributed to a pronounced Γ - L transfer in the drift region, since the simulation shows that a field strength of 1–10 kV/cm occurs in the drift region even in the low-conductivity state and of about 20–40 kV/cm in the high conductivity state, where strong thermionic emission dominates.

Now we present further simulations of the dynamic behavior. At first we note that the transit time of the electrons through the sample should be lower than 7 ps if we assume the average velocity to be larger than 10^7 cm/s. Therefore, it

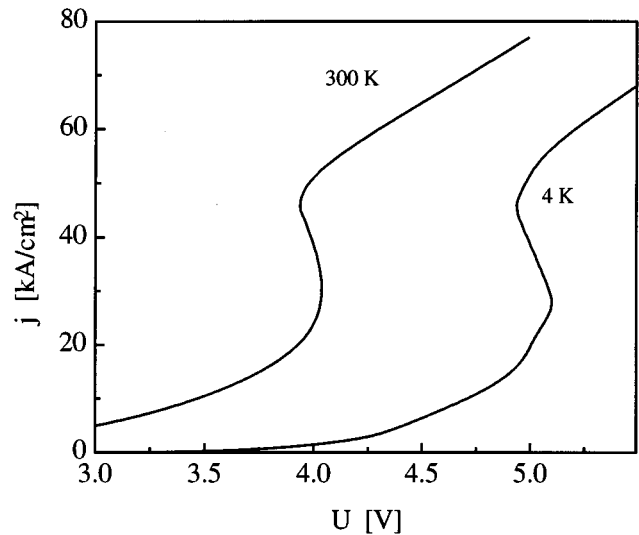


FIG. 6. Calculated current-voltage characteristics for different lattice temperatures for a GaAs/Al_{0.34}Ga_{0.66}As heterostructure hot electron diode. Both layer widths are 200 nm.

is reasonable to assume that the distribution of the electrons adiabatically follows the actual potential distribution. The potential distribution itself is strongly dependent on the (two-dimensional) charge density ρ_s in front of the heterojunction, which determines the difference of the electric fields inside the drift region and the barrier. This quantity can be identified to be the most relevant dynamical variable in the framework of the general treatment of Ref. 17. Therefore the dynamical behavior of the diode has been simulated by reducing the number of degrees of freedom to two essential dynamic variables, viz., the total voltage across the structure U and ρ_s .^{13,14} There it has been assumed that all charges are essentially free, so that their dynamics are governed by the continuity equation. This means that the change of ρ_s in time is just given by the difference of the current j_{GaAs} in the drift region and the current j_{AlGaAs} in the barrier. The calculated characteristic shows that ρ_s changes from $\rho_l = -2.3 \times 10^{-7}$ As/cm² at the low-conducting state to $\rho_h = -1.7 \times 10^{-7}$ As/cm² at the high-conducting state for $U = 5$ V, $T = 4$ K. The typical switching times should be of the order of $(\rho_h - \rho_l) / (j_{\text{GaAs}} - j_{\text{AlGaAs}})$. Assuming that the difference in the current densities ($j_{\text{GaAs}} - j_{\text{AlGaAs}}$) inside the sample is of the order of several percent of the total current, we obtain typical time scales which should be shorter than 100 ps. The numerical results for the total delay and switching times in dependence on the voltage are shown in Fig. 7. In agreement with our estimate we obtain times which are shorter than 100 ps except for voltages which are very close to the threshold voltage, where long delay times occur. Here the quantity $(j_{\text{GaAs}} - j_{\text{AlGaAs}})$ is almost zero as we are close to the stationary current-voltage characteristic where the condition of steady state gives $j_{\text{GaAs}} = j_{\text{AlGaAs}}$. The origin of the different delay and switching times can be understood in terms of a phase portrait analysis of the nonlinear dynamic system describing the threshold switching transitions.¹⁶ In the phase space of the dynamic variables the low- and high-

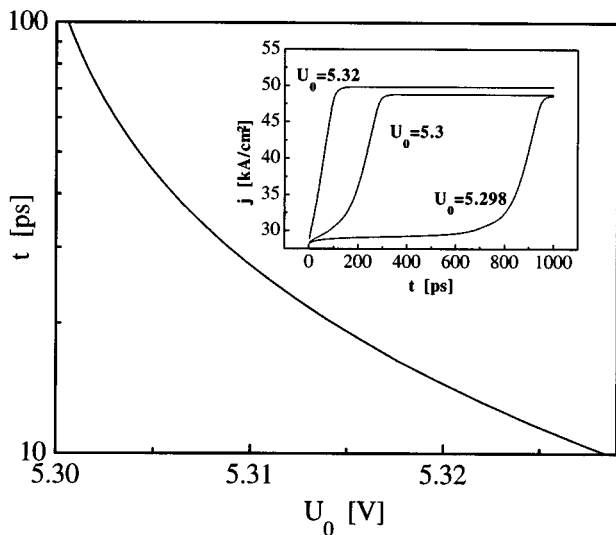


FIG. 7. Calculated total time for delay as a function of the applied voltage U_0 , where the device is operated in a circuit with a load resistor R . The inset shows the temporal evolution of the current for three different applied voltages ($T=4$ K, $R=50$ Ω , sample cross section $A=4\times 10^{-8}$ cm^{-2}).

conductivity states correspond to the stable fixed points. If the applied voltage is raised to a value above threshold, the low-conductivity state becomes unstable, and the system moves along a trajectory towards the high-conductivity state. For small overvoltages, the phase portrait is not changed much and the initial state is still influenced by the former stable fixed point; therefore the system will spend most of its time near the low-conductivity state before it eventually becomes faster along its trajectory towards the high-conductivity state. Thus the delay time is essentially determined by the phase portrait only in the neighborhood of the low-conductivity state, i.e., by the unstable linear eigenvalue of the corresponding fixed point, while the switching time is influenced by the global nonlinear features of the whole phase portrait between the two fixed points. This can explain the exponential decrease of the delay time with increasing overvoltage, as well as the much weaker dependence of the switching times upon varying overvoltage,¹⁶ as also observed in our experiments.

The theoretically determined delay and switching times are, by orders of magnitude, too fast, compared with the experiment. This discrepancy can certainly not be explained by the different sample parameters used, which might somewhat change the time scale, but it strongly indicates that the dynamical behavior is governed by additional effects neglected in the simulation. A possible explanation could be the presence of some unidentified electronic states, which become recharged during the switching process on a long time scale governed by their capture cross section and re-emission time. It is well known that in spite of carefully controlled growth conditions some 10^{10} cm^{-2} interface states are always present besides possible deep centers as well. It cannot be fully excluded furthermore that deep levels are created by ion implantation.

The role of charging additional electronic states is supported by using a double pulse technique and varying the time between two subsequently applied pulses. If the interval becomes short enough and the states have not been fully emptied in the meantime the switching occurs after a shorter delay time. However, the switching time remains the same as for single pulses.

V. SUMMARY

Our detailed experimental results clearly demonstrate the bistability in the single heterobarrier structure due to the abrupt transition between the tunneling and the thermionic emission regimes as proposed in Ref. 2. However, the bistability is persistent up to room temperature in contrast to Ref. 2. The theoretically predicted trend¹⁴ of the temperature dependence (Fig. 6) is correctly reflected in the experimental data, even if it is less pronounced for our structure (Fig. 3) due to the difference in scattering events in the long drift region as discussed above. The discrepancy between the theoretically expected and experimentally observed time-scales for delay and switching times may be related to electron capture at interface states or deep centers due to growth-related imperfections in contrast to the numerical simulation, which assumed that all electrons are free.

ACKNOWLEDGMENTS

We thank the colleagues from Ferdinand-Braun-Institute for ion implantation and performing the steps for the necessary preparation. Our thanks are also due to E. Wiebcke for support concerning the technological processing and to R. Klann for critically reading the manuscript. This work was partially supported by DFG in the framework of Sfb 296.

- ¹M. P. Shaw, V. V. Mitin, E. Schöll, and H. L. Grubin, *The Physics of Instabilities in Solid State Electron Devices* (Plenum, New York, 1992).
- ²K. Hess, T. K. Higman, M. A. Emanuel, and J. J. Coleman, *J. Appl. Phys.* **60**, 3775 (1986).
- ³T. K. Higman, L. M. Miller, M. E. Favaro, M. A. Emanuel, K. Hess, and J. J. Coleman, *Appl. Phys. Lett.* **53**, 1623 (1988).
- ⁴A. M. Belyantsev, A. A. Ignatov, V. I. Piskarev, M. A. Sinitsyn, V. I. Shashkin, B. S. Yavich, and M. L. Yakovlev, *Pisma Zh. Eksp. Teor. Fiz.* **43**, 339 (1986).
- ⁵T. K. Higman, J. M. Higman, M. A. Emanuel, K. Hess, and J. J. Coleman, *J. Appl. Phys.* **62**, 1495 (1987).
- ⁶C. Song and K. P. Roenker, *J. Appl. Phys.* **72**, 4417 (1992).
- ⁷Zh. I. Alferov, O. A. Mezrin, M. A. Sinitsyn, S. I. Troshkov, and B. S. Yavich, *Sov. Phys. Semicond.* **21**, 304 (1987).
- ⁸D. Arnold and K. Hess, *Appl. Phys. Lett.* **53**, 373 (1988).
- ⁹D. Arnold, K. Hess, T. Higman, J. J. Coleman, and G. J. Iafrate, *Appl. Phys. Lett.* **66**, 1423 (1989).
- ¹⁰A. Wacker and E. Schöll, *Appl. Phys. Lett.* **59**, 1702 (1991).
- ¹¹A. M. Belyantsev, E. V. Demidov, and Yu. A. Romanov, *Lithuanian J. Phys. Suppl.* **5**, 31 (1992).
- ¹²A. Reklaitis and G. Mykolaitis, *Solid State Electron.* **37**, 147 (1994).
- ¹³A. Wacker and E. Schöll, *Semicond. Sci. Technol.* **9**, 592 (1994).
- ¹⁴A. Wacker, Ph.D. thesis, Technical University, Berlin 1993.
- ¹⁵In practice the net switching time to some more or less arbitrary limits such as the 10% and 90% points of the steep rise. See G. C. Vezzoli, L. M. Doremus, S. Levy, G. K. Gaule, B. Lalevic, and M. Shoga, *J. Appl. Phys.* **52**, 833 (1981).
- ¹⁶E. Schöll, *Nonequilibrium Phase Transitions in Semiconductors* (Springer, New York, 1987).
- ¹⁷A. Wacker and E. Schöll, *J. Appl. Phys.* **78**, 7352 (1995).